LBL-22325
Preprint

Lawrence Berkeley Laboratory
UNIVERSITY OF CALIFORNIA

APPLIED SCIENCE DIVISION

RECEIVED
LAWRENCE
BERKELEY LABORATORY

APR 22 1987

LIBRARY AND
DOCUMENTS SECTION

Submitted to Building and Environment

A SIMPLIFIELD MODEL FOR PREDICTING AIR FLOW IN MULTIZONE STRUCTURES

H.E. Feustel and M.H. Sherman

February 1987

TWO-WEEK LOAN COPY

This is a Library Circulating Copy which may be borrowed for two weeks

APPLIED SCIENCE DIVISION

LBL-22325 c.2

Prepared for the U.S. Department of Energy under Contract DE-AC03-76SF00098

DISCLAIMER

This document was prepared as an account of work sponsored by the United States Government. While this document is believed to contain correct information, neither the United States Government nor any agency thereof, nor the Regents of the University of California, nor any of their employees, makes any warranty, express or implied, or assumes any legal responsibility for the accuracy, completeness, or usefulness of any information, apparatus, product, or process disclosed, or represents that its use would not infringe privately owned rights. Reference herein to any specific commercial product, process, or service by its trade name, trademark, manufacturer, or otherwise, does not necessarily constitute or imply its endorsement, recommendation, or favoring by the United States Government or any agency thereof, or the Regents of the University of California. The views and opinions of authors expressed herein do not necessarily state or reflect those of the United States Government or any agency thereof or the Regents of the University of California.

LBL-22325

Submitted for publication to *Building and Environment*

A SIMPLIFIED MODEL FOR PREDICTING AIR FLOW IN MULTIZONE STRUCTURES

Helmut E. Feustel and Max H. Sherman

Indoor Environment Program

Lawrence Berkeley Laboratory

University of California

Berkeley, California 94720, U.S.A.

February 1987

This work was supported by the Assistant Secretary for Conservation and Renewable Energy, Office of Building Energy Research and Development, Building Systems Division of the U.S. Department of Energy under Contract No. DE-AC03-76SF00098.

Abstract

Several infiltration models exist to treat air flows in multizone buildings. Most of them, however are written as research tools and rely on the use of mainframe computers; as such, they are generally unavailable to the average user. Even if they can be obtained, the models are seldom user-friendly. Engineers and architects are key professionals in need of a simplified multizone infiltration model that will allow them to predict infiltration and ventilation for buildings. This paper describes the second step in the development by Lawrence Berkeley Laboratory (LBL) of a multizone infiltration model for calculating the air-flow distribution of a complex building. This model is based on an algorithm that can be determined with a pocket calculator. To simplify the calculation process, we have categorized buildings on the basis of their ratio of permeabilities and have lumped together the physical parameters describing the air permeability distribution needed to calculate the building's overall infiltration/exfiltration rate. The simplified multizone model described in this paper is illustrated by a sample calculation of an eight-story building.

Keywords: Multizone Infiltration, Air-Flow Modeling, Lumped Parameters.

1. Table of Symbols

a	crack coefficient [$m^3/mhPa^n$]
c_k	pressure coefficient for surface element k [-]
$\bar{c}_{lee}$	average pressure coefficient on the leeward side [-]
$\bar{c}_{wind}$	average pressure coefficient on the windward side [-]
dp	pressure gradient [Pa]
dv	velocity gradient [m/s]
dz	height gradient [m]
g	acceleration of gravity [m/s^2]
h	height of the building [m]
j	number of considered story [-]
k	number of stories [-]
l	crack length [m]
lee	leeward side
luv	windward side
m	air mass flow [kg/h]
n	exponent of the pressure difference [-]
p	pressure [Pa]
p_0	atmospheric pressure [Pa]
p_{dyn}	dynamic pressure in the undisturbed flow [Pa]
p_{in}	inside pressure [Pa]
p_k	pressure at surface element k [Pa]
p_{out}	outside pressure [Pa]
Δp_{stack}	pressure difference due to stack [Pa]
Δp_{tot}	pressure difference due to stack and wind action [Pa]
Δp_{wind}	pressure difference due to wind [Pa]
$sign$	sign of the following expression [-]
$t_{in}; t_{out}$	temperature inside; outside [° C]
v	wind speed [m/s]
x, y, z	coordinates [m]
z_n	neutral pressure level [m]
z_r	roughness height, depends on terrain roughness [m]
z_{ref}	reference height for former calculation [m]
z_0	reference height for wind velocity measurements [m]
D	air permeability of the building component [$m^3/h\ Pa^n$]

D_{lee}	air permeability of the leeward side of the building envelope $[m^3/h\ Pa^n]$
D_{ref}	resultant permeability at reference conditions $[m^3/h\ Pa^n]$
D_{res}	resultant permeability $[m^3/h\ Pa^n]$
D_{shaft}	air permeability from the story to the shaft $[m^3/h\ Pa^n]$
D_{total}	air permeability of the total building envelope $[m^3/h\ Pa^n]$
Q	air flow through a building component $[m^3/h]$
Q_{ref}	air flow at reference conditions $[m^3/h]$
Q_{tot}	superimposition of flows $[m^3/h]$
Q_{wind}	air flow due to wind $[m^3/h]$
Q_{stack}	air flow due to temperature differences $[m^3/h]$
Re	Reynolds number [-]
α	exponent [-]; value depends on terrain roughness
ϕ	wind direction [°]
ρ_{out}	density of the outside air $[kg/m^3]$
ρ_{in}	density of the inside air $[kg/m^3]$

2. Introduction

A number of computer programs have been developed to calculate infiltration-related energy losses and the resultant air flow distribution in buildings (see Ref. [1]). Awareness of the air flow pattern in a building is particularly important when determining indoor air quality problems for the different zones in a building, smoke distribution during a fire, and space conditioning loads for calculating energy consumption. The correct sizing of necessary space conditioning equipment is also dependent upon accurate air flow information.

If the true complexity of air flows brought about by climatic variables is to be properly treated in multizone buildings, extensive information regarding flow characteristics and pressure distribution inside and outside the building is essential.

Mainframe computers are the standard hardware used to host models designed to solve the set of nonlinear equations created by air flow patterns through building components. To reduce the necessary input data required by detailed infiltration models, researchers have developed a variety of simplified models. Most of these models, including the one developed at the Lawrence Berkeley Laboratory [2], simulate infiltration associated with single-cell structures. (Air flow in a building that can be described as one fully-mixed space without any internal flow restrictions and no pressure gradients in the horizontal direction can also be calculated by using single-cell infiltration models.)

A high percentage of existing buildings, however, have floor plans that characterize them more accurately as multizone structures. Although multizone models exist, the vast majority (1) are not readily available to the end user and (2) are written as research tools requiring inordinate amounts of input data to describe the external pressure distribution and air permeability distribution of the building [1]. Furthermore, to determine the impact of infiltration and air flow patterns within buildings, engineers and architects need a simplified multizone infiltration model. In this paper, the second steps towards developing such a model are explained and preliminary results are provided.

2.1 Modeling Strategies

For any detailed infiltration model, buildings can be viewed as an interlaced grid of flow paths [3]. In this grid system, the joints are the zones of the building, and the connections between the joints simulate the flow paths. The grid also illustrates flow resistances caused by open or closed doors and windows and/or other air leakage paths through the walls. The grid points outside the building mark the boundary conditions for wind pressure. Differences in air density, caused by differences between outside and inside air temperatures, create additional pressures in the vertical direction, and these pressures also influence a building's air flow.

Table 1: Comparison of modeling strategies		
Model	Advantage	Disadvantage
single-cell	easy to handle, requires few input data, provides reasonable accuracy	simulates only single cell structures; i.e., no internal flows or partitions
detailed	useful for larger buildings, measures internal flows, has good accuracy	requires extensive input and mainframe computer
simplified multizone	very useful for larger buildings, measures internal flows, is easy to use, requires reduced input, can be calculated on pocket calculator	reduced accuracy

In buildings with mechanical ventilation systems, the duct system can be treated as another interior flow path, the fan being an additional source of pressure difference. The fan lifts the pressure level between two joints according to the characteristic curve of the fan. The HVAC components, such as heating and cooling coils, constitute sources of pressure loss. Due to the nonlinear dependency of the flow on the pressure difference, the pressure distribution is generally calculated in several iterations. For detailed multizone infiltration models describing buildings with complicated floor plans and solving the resulting set of nonlinear equations, a computer with a large storage capacity is needed. From the simplified multizone infiltration model described together with the superimposition of flows obtained from the application of the lumped parameters, one can calculate the air flow through multizone buildings.

3. Physical Fundamentals of the Pressure Distribution

For free-stream, nonviscous flow, the Bernoulli equation provides the relationship between the pressure, the velocity, and the density of the fluid:

$$dp + \rho\ v\ dv + \rho\ g\ dz = 0 \tag{1}$$

This equation is quite important for gaining an understanding of fluid behavior in any given structure [4].

3.1 Wind Pressure

Wind flows produce a velocity and pressure field around buildings. The relationship between velocity and related pressure at different locations of the flow field can be obtained from the dynamics of a particle in the fluid. For free-stream flow, solving Bernoulli's equation provides the relationship between the pressure,

density and the velocity field. Bernoulli assumes steady-state flow in a regime where viscous forces are negligible. By integrating Eq. 1 one gets:

$$p + \frac{1}{2}\,\rho\,\vec{v}^2 + \rho g z = const. \tag{2}$$

For wind-flow problems, the gravitational term of the equation is negligible in most cases. When compared to the static pressure associated with an undisturbed wind-velocity pattern, the pressure field around a building is generally characterized by regions of overpressure on the windward side (drop of velocity), and underpressure on the facades parallel to the air stream and on the leeward side.

The pressure distribution around a building is usually described by dimensionless pressure coefficients — the ratio of the surface pressure and the dynamic pressure to the undisturbed flow pattern:

$$c_k(x,y,z,\phi) = \frac{p_k(x,y,z) - p_0(z)}{p_{dyn}(z)} \tag{3}$$

with

$$p_{dyn}(z) = \frac{1}{2}\,\rho_{out}\,v^2(z) \tag{4}$$

The shear layer formed by the action of shear stress at a solid boundary is called a boundary layer. The velocity in that shear layer goes from zero at the surface of the solid boundary up to the velocity of the free stream at the outer edge. The flow in the region between these limits is dominated by the effect of viscosity. Depending upon the Reynolds number, the flow in this region is either laminar or turbulent. Wind flow is characterized by turbulent boundary layer flow having a thickness of a few hundred meters.

The vertical profile of the wind speed in the atmospheric boundary layer depends primarily upon the roughness of the surfaces surrounding the building. The wind speed increases with increasing height above ground. The wind velocity profile can be calculated either by a logarithmic equation or a power law expression, as in (5) and (6) respectively.

$$\frac{v(z)}{v(z_0)} = \frac{\ln\left\{\dfrac{z}{z_r}\right\}}{\ln\left\{\dfrac{z_0}{z_r}\right\}} \tag{5}$$

or

$$\frac{v(z)}{v(z_0)} = \left\{\frac{z}{z_0}\right\}^{\alpha} \tag{6}$$

The latter is most often used by engineers and building scientists.

These equations assume that the wind flow is isothermal and horizontal, and that the wind flow will not change its direction as a result of differences in the terrain surface. The value of the exponent α increases with increasing roughness of the solid boundary. For smaller areas of rough surfaces in smoother surroundings, such as a town located in flat, open country, the velocity profile described by Eqs. 5 and 6 is valid only for a limited height above the obstacles. The wind velocity above the zone is determined by the roughness of its surroundings.

3.2 Thermal Buoyancy

Temperature differences between the outside and inside air create air density differences that cause pressure gradients. The stack-effect pressure gradient depends only upon temperature differences and the vertical dimension of the structure [7,8,9]. This effect is often misunderstood to be a form of convection; however, temperature differences within the two columns of air do not cause this phenomenon. The effect deals with the weight difference between the two adjacent columns of air. Buoyancy forces try to even out these differences, causing an overpressure at the top of the warm column of air and an underpressure at the bottom. The value of pressure differences in high-rise buildings located in cold climates can easily exceed those caused by wind effects. The theoretical value of the pressure difference depends on the gradient and distance of the neutral pressure level (z_n), defined as the height on the building facade where, under calm conditions, no pressure difference exists between inside and outside. The vertical permeability distribution of the envelope determines the location of the z_n. The stack effect (or thermal buoyancy) can be calculated by integrating Bernoulli's equation assuming no wind:

$$d(p_{out} - p_{in}) = g\,(\rho_{in} - \rho_{out})\,dz \tag{7}$$

and, after integration,

$$(p_{out} - p_{in})_{stack} = g\,(\rho_{in} - \rho_{out})\,(z - z_n) \tag{8}$$

4. Air Flow through the Structure

The permeability of a building's envelope is dependent upon the number of cracks, windows, doors, and gaps between building components. In addition to these visually observable leaks, there is also background leakage caused by the porosity of building material and cracks in these materials. Leakage measurements of building components and wall sections were reported as early as the 1920's. (See Brinkmann [10]; for current articles on air flows through cracks, see Kronvall [11]

and McGrath [12].) Measurement data on air permeability in building components is, for the most part, described by the empirical power-law equation:

$$Q = (a\ l)\ \Delta p^n = D\ \Delta p^n = D\ (p_{out} - p_{in})^n \tag{9}$$

The air flow through a structure can be measured by the fan pressurization technique using a blower door (DC) [13] or the AC pressurization technique [14]. From these data, the air permeability, D, and the exponent of the pressure difference, n, can be determined. The value of the exponent n is expected to be between its physical limits of $n = 1.0$, for fully developed laminar flow, and $n = 0.5$, for fully developed turbulent flow. A comparison of air leakage in 196 houses, measured by the blower door technique (DC), produced a mean exponent value of 0.66 [15]. This finding is in agreement with the measured flow characteristic, n, of building components [16,17].

5. Air Flow Distribution

5.1 Air Flow Due to Temperature Differences

Under calm conditions, the difference in thermal pressure for a given temperature difference is a linear function of the distance of the height above ground from the neutral pressure level (z_n) (see Eq. 8). The volume rate driven by thermal buoyancy alone is:

$$Q_{stack}(z) = sign(\Delta p_{stack})\ D_{res}(z)\ \left|\Delta p_{stack}(z)\right|^n \tag{10}$$

$$\Delta p_{stack} = (p_{out} - p_{in})_{stack} \tag{11}$$

$D_{res}(z)$ is the resultant permeability calculated for the arrangement of permeabilities in series or in parallel to the place where the stack pressure occurs (elevator shaft, stairwell, etc.) and the outside. For an apartment building, these permeabilities could consist of elevator doors, doors to individual apartments, interior apartment doors, and openings of facades. In addition to the pressure gradient in shafts and vertical ducts, there is the same buoyancy effect at each individual story of the building. Because of the limited height of the story and the relatively small distances of the different openings from the local z_n of the story, these pressure differences may be negligible when compared to those forced by wind and the chimney effect of internal shafts.

5.2 Air Flow Due to Wind

To calculate air pressure differences caused by wind, one must determine the outside pressure field as well as the internal pressure distribution. Detailed multizone infiltration models usually calculate the flow distribution of an air mass by solving the continuity equation for each zone using Eq. 9 and changing the pressure distribution inside the building in an iteration procedure. The set of nonlinear

equations produced is usually solved by using Newton's method of iteration.

The internal pressure is a function of the permeability distribution of the building's envelope and of the internal flow resistances. From the continuity equation the air flow for each story can be derived:

$$\rho_{out}\, D_{wind}(z)\, [\Delta p_{wind,windward}(z,\phi,T)]^n = \rho_{in}\, D_{shaft}(z)\, [p_{in}(z) - p_{shaft}]^n$$

$$+ \rho_{in}\, D_{lee}(z) \left\{ \Delta p_{in}(z) - [p_{dyn}(z)\, \bar{c}_{lee}(z,\phi)] \right\}^n \tag{12}$$

In this case the permeability D_{wind} results from adding all of the flow paths existing between the facade of the windward side and the reference point. This same calculation must be performed for the leeward side. For buildings with no permeability between different stories (story-type buildings), this set of equations can be solved independently for each story. For all other types of buildings this set of equations has to be solved by using a method of iterations.

The inside pressure distribution due to wind will become uniform with an increasing permeability from the stories to the shaft. The pressure difference responsible for the wind-driven air flow can be calculated by:

$$\Delta p_{wind,windward}(z,\phi,T) = \frac{\rho_{out}}{2} \left\{ v(z_0) \left[\frac{z}{z_0} \right]^{\alpha} \right\}^2 \bar{c}_{wind}(z,\phi) - \Delta p_{in}(z) \tag{13}$$

This pressure difference is mainly a function of the wind speed at reference height, the building surroundings, the building's height above ground and the building type. The volume rate driven by wind action alone can be calculated by:

$$Q_{wind}(z,\phi) = D_{wind}(z)\, [\Delta p_{wind,windward}(z,\phi)]^n \tag{14}$$

6. Simplification

6.1 Overview

To simplify the calculation procedure, we adopted the following measures as noted earlier. We defined a set of lumped parameters to describe the permeability distribution of the building, used a single exponent for the pressure distribution, calculated the wind- and stack-driven air flows separately, and used superimposition to combine the air flows.

6.2 Resultant Permeability

The effective air permeability for a building is most often a combination of air permeabilities arranged in series and/or in parallel. Parallel permeabilities can be easily added, but for a series arrangement permeability has to be calculated thusly:

$$Q = D_{res} \left\{ (p_1 - p_2) + (p_2 - p_3) + \cdots + (p_{k-1} - p_k) \right\}^n \tag{15}$$

$$Q = D_1 (p_1 - p_2)^n = D_2 (p_2 - p_3)^n = D_{k-1} (p_{k-1} - p_k)^n \tag{16}$$

$$D_{res} = \left\{ D_1{}^{-1/n} + D_2{}^{-1/n} + \cdots + D_{k-1}{}^{-1/n} \right\}^{-n} \tag{17}$$

The use of these equations assumes that all permeabilities have the same flow characteristics and the same exponent, n. Figure 1 illustrates resultant air permeability for two resistances in a series arrangement with exponent n=2/3.

6.3 Superimposition of Flows

Air flows caused by separate mechanisms (such as wind and thermal buoyancy) are not additive because the flow rates are not linearly proportional to the pressure differences. To superimpose the flows, adding the pressures is required. The superimposed volume rate can be calculated by:

$$Q_{tot} = D\,(\Delta p_{tot})^n \tag{18}$$

$$Q_{tot} \approx D\,(\Delta p_{wind,horizontal} + \Delta p_{wind,vertical} + \Delta p_{stack})^n \tag{19}$$

$$Q_{tot} \approx (Q_{wind,horizontal}{}^{1/n} + Q_{wind,vertical}{}^{1/n} + Q_{stack}{}^{1/n})^n \tag{20}$$

Because each mechanism may force the air to flow in a different direction, the superimposition of flows for each facade and story is expressed as:

$$Q_{tot} = sign(Q_{wind,horizontal} + Q_{wind,vertical} + Q_{stack}) \times$$

$$\left| \left[sign(Q_{wind,horizontal}) \mid Q_{wind,horizontal} \mid^{1/n} + \right.\right.$$

$$sign(Q_{wind,vertical}) \mid Q_{wind,vertical} \mid^{1/n} +$$

$$\left.\left. sign(Q_{stack}) \mid Q_{stack} \mid^{1/n} \right] \right|^{n} \tag{21}$$

Fig. 2 shows that both driving forces for natural ventilation can be calculated separately and superimposed to obtain the total natural ventilation.

6.4 Lumped Parameters

To describe the air flow distribution inside a building we introduced five lumped parameters reflecting the different permeability distributions of the building's envelope and flow resistances inside the building. Krischer and Beck [18] used the following parameter to describe the envelope permeability ratio (*epr*) of the whole building:

$$epr(\phi) = \frac{D_{lee,envelope}}{D_{total,envelope}} \tag{22}$$

The influence on the resultant permeability of a structure and its infiltration is shown in Fig. 3. For a given permeability of the total envelope, the infiltration rate reaches its maximum at an envelope permeability ratio of 0.5 (typical row house) due to the fact that the value of the resultant permeability is governed by the smallest permeability in a series arrangement. Therefore, for buildings whose air permeabilities are distributed unevenly between the leeward and the windward side, the infiltration will be smaller. The wind-driven infiltration under steady-state conditions will be zero if all air permeability is located on either side.

Figure 4 shows the related internal pressure depending on the envelope permeability ratio *epr* for one story in a story-type building for two different wind directions in case of $t_{in} = t_{out}$ and $\bar{c}$ according to recommendations given by Krischer and Beck [18].

The most current issue of the German standard for calculating heat loss in buildings, DIN 4701 [19], introduces another parameter to further differentiate construction types. Based on this parameter we introduced the ratio of the permeabilities from one floor to another, and the overall permeability of the building envelope. Equation 23 describes the vertical permeability ratio (*vpr*) for a whole building of any given construction type.

$$vpr = \frac{D_{shaft}}{D_{total,envelope} + D_{shaft}} \tag{23}$$

With regard to thermal pressure distribution, two extremes exist — *story-type buildings* with no permeability between floors ($vpr = 0$), and *shaft-type buildings* with no air-flow resistance between the different stories ($vpr = 1$). The vertical permeability ratio for real houses is somewhere between these theoretical limits.

To describe the air-flow distribution for the different zones at the story level, we defined two additional lumped parameters [20,21]. The first lumped parameter is the outside permeability ratio (opr) of the zone. It describes the influence on cross-ventilation of the zone, where cross-ventilation is the portion of the air flow that exfiltrates the same zone it infiltrates. The second lumped parameter is the inside permeability ratio (ipr) of the zone. It describes the stack influence on the zone.

$$opr(\phi) = \frac{D_{zone,lee,outside\ envelope}}{D_{zone,outside\ envelope}} \tag{24}$$

$$ipr = \frac{D_{zone,shaft}}{D_{zone,outside\ envelope} + D_{zone,shaft}} \tag{25}$$

In a previous study using a detailed multizone infiltration model, a strong relationship appeared between the two latter ratios and the flow distribution in buildings [20]. With increasing values for opr and decreasing values for ipr, the zones became wind-dominated to a greater extent. Consequently, increasing ipr's in combination with decreasing opr's resulted in just the opposite effect.

During the second development phase of this model, it was determined that the internal air flows in a building due to wind are directly dependent upon the ratios of the resultant permeabilities of the different zones. These are defined as the combination of all flow paths (parallel and series arrangements) from this zone to either the windward or leeward side of the building. The resultant permeability ratio (rpr) is the ratio of the resultant permeability of the downstream side to all resultant permeabilities of this particular zone. The permeability ratio contains all information given by the outside permeability ratio together with all the flow paths not directly leading to the outside of the building.

$$rpr(\phi) = \frac{D_{res,zone,lee}}{D_{res,zone,total}} \tag{26}$$

Determining the resultant permeabilities is far more complicated than determining the permeabilities used for the other four ratios. The majority of the permeabilities have to be shared by different flow paths. Calculating the resulting permeability ratio for the internal flows may require an iteration procedure.

6.5 Air Flow Due to Thermal Buoyancy

Calculating the air flow caused by the stack effect is very simple. A measure to further simplify the calculation procedure is described in Ref. 22 and shall not be repeated here. Instead, it is recommended that Eqs. 10 and 11 be used.

6.6. Air Flow Due to Wind Action

6.6.1 Introduction

In using this simplified model to calculate the air flow due to wind, it is convenient to distinguish among different cases based on the type of floor plan. The simplest case would be to treat each story as a single-cell. The second case, somewhat more complicated, is represented by buildings with zones that have air permeabilities either on the windward side or on the leeward side, but not both. Still more complicated are those buildings having zones with openings to the windward side and the leeward side without being treatable as single-cell stories.

6.6.2 Single Cell Approach

For all buildings, the upper limit for the overall infiltration rate can be calculated by using the single-cell approach for each story in a story-type building. The infiltration can be easily calculated by using the resultant permeability ratio from Fig. 3 and the proposed wind pressure as input data. This procedure works on all types of buildings. If the building is not a story-type building, the air flow calculation will give low values for the upper floors and high values for the lower floors. The sum for the whole building, however, approximates the actual infiltration value for the building. These simple calculations are very helpful in cases where the local infiltration rate is not of interest; i.e., when the primary concern is to design boiler sizes for central heating systems.

6.6.3 Vertical Air Flow Due to Wind

Besides determining the permeability distribution and the pressure field around the building, the most difficult aspect of calculating wind-driven infiltration is determining the inside pressure distribution of the house. In addition to the air flows caused by stack effects, different wind speeds at different heights also cause air flows through the shafts of a building. Air flows due to stack action travel upwards most of the time ($t_{in} > t_{out}$). In high buildings air flows are forced by wind from the top to the bottom of the building.

Because the air flow through the shaft due to wind action and thermal buoyancy causes no significant friction losses in the staircase, it can be assumed to have no pressure gradient inside the shaft itself; that is, the distribution of the shaft leakage over the height of the shaft can be assumed to be uniform. This, in conjunction with Eq. 27, can be used to calculate the pressure of the shaft as a first approximation, as shown in Eq. 28:

$$0 = \sum_{j=1}^{k} \left\{ sign(p_{in,j} - p_{shaft}) \left| p_{in,j} - p_{shaft} \right|^{n} \right\} \approx \sum_{j=1}^{k} \left\{ p_{in,j} - p_{shaft} \right\} \tag{27}$$

$$p_{shaft} = \frac{1}{k} \sum_{j=1}^{k} p_{in,j} \tag{28}$$

For this calculation, the inside pressures of story-type buildings may be used.

A further simplification for calculating the pressure of the shaft would be to use the average of the inside pressures for the top and bottom stories.

$$p_{shaft} = 1/2 \left\{ p_{in,j=1}(epr, vpr{=}0) + p_{in,j=k}(epr, vpr{=}0) \right\} \tag{29}$$

This calculation gives slightly different values for the shaft pressure compared to the calculation presented in Eq. 28. It uses the inside pressure from Fig. 4 for buildings with the *epr* as input. This calculation assumes story-type buildings with a central corridor, a symmetrical floor plan, and certain surface pressure coefficients of $c_{wind} = 1.0$ for the windward side, $c_{lee} = -0.3$ for the leeward side, and perpendicular air flow [18]. For buildings having more complicated floor plans, Fig. 4 can be used with the *rpr* of the floor's landing as an input. How to calculate the resultant permeability ratio is described in paragraph 6.2.

A comparison of different infiltration models [1] revealed the importance of air flow through the shaft, even when no stack effect is present. The high pressures at the top of the building cause a downstream of infiltrated air in the shaft and this air is released into the lower levels of the building. This has a significant effect on the flow distribution of houses having small *epr* values. The following empirical equation yields the approximate value for the inside pressures as a function of the building's height above ground and the building type.

$$p_{in}(z) = p_{shaft} + \frac{2}{h} \left\{ p_{in}(z{=}h, epr, vpr{=}0) - p_{shaft} \right\} (1 - vpr^{n}) (z - h/2) \tag{30}$$

With these assumptions, the inside pressure distribution necessary for calculating wind-driven air flow using Eqs. 13 and 14 can be determined.

6.6.4 Air Flow in Buildings with Complex Floor Plans

The wind action for buildings with simple floor plans (as shown in [22]) can be treated by using Eqs. 14 and 30, but buildings with complex floor plans create difficulties. In these cases, the introduction of an iteration procedure may be necessary.

To avoid calculating pressure distribution inside the building, one can determine the air flow path through each of the stories using the story-type building as a base case. The air-flow compensation of the different stories due to given vertical air permeability and downdraft of the air flow caused by different wind speeds at different heights above ground can be managed by using the equations given in section 6.6.3.

Determining the air-flow path through a building for a given wind direction requires examining the floor plan for all possible paths from the windward side to the leeward side of the building. Knowing that air flows from zones with low *rpr* values to those with high *rpr* values allows the flow direction to be determined. For the initial values of the iteration procedure, *rpr* values can be replaced by their *opr* counterparts.

The portion of air permeability used by different flow paths can be determined by splitting the single permeability by the same ratio as the two parallel permeabilities. A single permeability on the windward side of the building which is used by flow paths through two different permeabilities on the leeward side can be split according to Eq. 31.

$$D_{wind,1} = D_{wind,total} \frac{D_{lee,1}}{D_{lee,1} + D_{lee,2}} \tag{31}$$

Combining permeabilities is, for the most part, not as simple as the above would suggest. The resultant air permeability of a flow path may be a combination of series and parallel arrangements passing through a series of different zones. For permeabilities used by flow paths all traveling through one more zone (where there is no direct-through flow), the parallel portion of the permeability can be calculated using the *rpr* differences as a measure of the different zones involved in the flow paths. The portions of the permeability D_l located in zone l for zone k with the resultant permeability ratio rpr_k can be calculated using the following expression:

$$D_k = \frac{(rpr_k - rpr_l)\, D_l}{\sum_j (rpr_j - rpr_l)} \tag{32}$$

The air flows for each flow path can then be directly calculated using the resultant permeabilities as inputs to Eq. 9.

7. Example

Figure 5 shows the floor plan of an eight-story building with three flats per story. (The calculation procedure for a simple floor plan was shown in a previous paper [22].)

The envelope permeability ratio (epr) calculates to:

$$epr = \frac{D_{lee,envelope}}{D_{total,envelope}} = \frac{37.3}{81.2} = 0.459$$

From Eq. 9 and Fig. 3 we can determine the overall infiltration rate due to wind, using the permeability values given in Table 3.

Table 3: Permeabilities for different zones of the building (wind direction = west)

Zone	Location	Permeability $[m^3/(h\ Pa^n)]$
1	windward	4.3
	leeward	8.6
	door	18.0
2	windward	0.0
	leeward	11.6
	door	18.0
3	windward	19.6
	leeward	17.1
	door	18.0
4	windward	20.0
	leeward	0.0
	doors	18.0

For the first story of a story-type building at wind speeds of 4m/s and a pressure distribution determined according to Krischer and Beck [18], an infiltration rate of $Q = 133\ m^3/h$ results. This value is only 3.8% higher than the value calculated by means of a detailed infiltration program that takes the internal partitions into consideration. The differences in the overall infiltration for the whole building are even less pronounced than the differences for a single story. When the overall infiltration rate due to wind is calculated for the same house but calculated as a shaft-type building, the result is only 0.3% lower than the rate calculated for the story-type building (see Table 4).

Table 4: Overall infiltration rates due to wind (in m^3/h) for floor plan shown in Fig. 5 at $v_{10} = 4m/s$, $\alpha = 1/3$ and wind pressure distribution given in [18]

Case	Simplified model	Detailed model	Difference in %
1st floor, story-type	133	128	3.8
8th floor, story-type	185	183	1.1
total bldg., story-type	1205	1175	2.6
total bldg., shaft-type	1205	1172	2.8

Calculating the infiltration for the different zones is more intricate. For wind blowing from the west, the permeability values are those given in Table 3. The *opr* values calculate to 0.667 for Flat No. 1, 1.0 for Flat No. 2, 0.446 for Flat No. 3, and 0.0 for the staircase (No. 4). The first step is to find the different flow paths for each story, keeping in mind that air flows from zones with low *rpr*-values to those with high *rpr*-values. We begin with the case of a building having no connection between the different floors ($vpr = 0.0$). The flow paths for such a building, using *opr* values as initial values for the *rpr*, are illustrated in Fig. 6.

The results for the different iterations show few differences in the air mass flow for the different flow paths, excepting the flow path for the door at flat No. 3 (see Table 5). Even though this mass flow changes about 50% in the five iteration steps, the change of the total through-flow due to wind for Flat No. 3 is only 2.5%. If the total air flow per zone is of more concern to the user than the air flow for a particular flow path, the first iteration step already gives a reasonable result. If the values for a particular flow path are important, however, the number of iteration steps required is determined by the smallest *rpr* difference.

The results of a simulation run using the simplified model for $v_0 = 4m/s$, an outdoor temperature of $t_{out} = -10\ ^\circ C$, and a building height of eight stories are shown in Table 6. The values represent the superimposition of the mass flows caused by wind and stack action. Compared with the values given for the wind effect in a story-type building on the ground floor level, some changes in the flow direction are caused by the strong stack effect. The comparison between the detailed and simplified models shows good agreement for most of the air flow path in the building; however, for flow paths with very low values for the mass flows, significant percentage differences can occur (see Table 7).

Table 5: Results for air mass flows due to wind at different iteration steps (in kg/h) for the first floor; $v_{10} = 4m/s$, $\alpha = 1/3$, $t_{out} = t_{in} = 20\ ^{\circ}C$ and wind pressure distribution given in [18]

Iteration Step	Flat #1 Luv	Flat #1 Lee	Flat #1 Door	Flat #2 Door	Flat #3 Door	Flat #3 Lee	Flat #3 Luv
#1	15.7	-35.8	20.1	35.5	13.2	-77.1	63.9
#2	15.8	-35.0	19.2	37.5	10.8	-76.0	65.2
#3	16.1	-35.3	19.2	37.8	10.5	-76.2	65.7
#4	16.0	-35.2	19.2	38.7	9.4	-75.5	66.1
#5	15.9	-35.4	19.5	38.7	8.8	-75.2	66.4
detailed model	16.0	-35.4	19.4	39.4	7.8	-75.0	67.2

Table 6: Results for air mass flows due to wind and stack using the simplified model in kg/h; $v_o = 4m/s$, $\alpha = 1/3$, $t_{out} = -10\ ^{\circ}C$ and wind pressure according to [18]

Story	Flat #1 Luv	Flat #1 Lee	Flat #1 Door	Flat #2 Door	Flat #3 Door	Flat #3 Lee	Flat #3 Luv
1	32.7	13.0	-59.3	-36.4	-106.2	-58.8	107.0
2	28.7	-13.2	-43.1	-15.1	-82.1	-68.1	98.1
3	24.3	-27.3	-22.7	21.8	-53.7	-76.8	88.6
4	20.1	-38.9	15.8	41.3	-14.6	-86.7	80.7
5	18.4	-51.1	36.3	58.5	36.9	103.1	82.1
6	16.3	-61.9	52.1	73.3	63.8	-117.7	82.7
7	13.9	-71.6	65.8	86.6	86.1	-131.1	82.6
8	11.1	-80.6	78.3	98.9	105.9	-143.5	82.1

8. Summary

Buildings are classified into different categories based on their air permeability distribution. This procedure is helpful in reducing the input data and limiting the different cases that might occur. The example given above shows the importance of the compensatory air flow between stories when only wind action is present. Models that restrict air flow due to wind action to the story under consideration miss an important part of the air-flow distribution in a building. The results

Table 7: Differences in mass flows between the detailed and the simplified model (in %)*; $v_o = 4m/s$, $\alpha = 1/3$, $t_{out} = -10\ ^oC$ and wind pressure according to [18]

Story	Flat #1 Luv	Flat #1 Lee	Flat #1 Door	Flat #2 Door	Flat #3 Door	Flat #3 Lee	Flat #3 Luv
1	-4.8	-3.2	19.3	11.0	16.3	13.5	-16.0
2	-9.7	18.9	58.2	81.9	17.3	12.4	-15.3
3	-8.0	10.2	79.2	12.8	17.6	10.3	-13.1
4	-0.5	0.5	-6.7	-2.4	15.0	4.7	-4.6
5	1.6	0.0	5.7	0.7	8.3	-1.1	5.9
6	2.6	0.5	8.4	2.1	11.4	-2.5	9.9
7	3.4	0.8	8.9	2.7	12.6	-3.0	12.3
8	4.2	1.4	8.3	3.2	11.6	-3.0	14.1

* Base case for the calculation is the total through-flow for each of the zones.

show that by adding the pressures, the air flow due to wind action and the air flow due to stack effect can be calculated separately and superimposed later.

In most infiltration models, two important parameters — the pressure field around the building and the permeability distribution of the external and internal building components — are usually estimated only roughly. Both of these parameters must be determined for proper evaluation and application of models. With the growing proliferation of wind tunnel studies, it may soon be possible to predict the pressure field around a building. The need remains, however, for a multizone pressurization method capable of yielding critical information about a building's air permeability distribution. Until both of these input parameters can be determined, all multizone infiltration models will be severely handicapped.

In our continuation work at LBL, we intend to focus on the air-flow distribution between different zones using *opr* and *ipr* as guiding principles. One immediate goal is to be able to calculate the air flow even when the wind direction is not perpendicular to the windward side of the building. Generally speaking, we believe that the problems that presently limit our ability to simulate infiltration in complex multizone structures deserve international attention.

9. Acknowledgements

This work was supported by the Assistant Secretary for Conservation and Renewable Energy, Office of Building Energy Research and Development, Building Systems Division of the U.S. Department of Energy under Contract No. DE-AC03-76SF00098.

10. References

[1] Feustel, H.E. and Kendon, V.M.:
Infiltration Models for Multicellular Structures - A Literature Survey
Lawrence Berkeley Laboratory, Report No. LBL 17588, (1985).

[2] Sherman, M.H.:
Air Infiltration in Buildings
Lawrence Berkeley Laboratory, Report No. LBL 10712, (1980).

[3] Feustel, H.E.:
"Beitrag zur theoretischen Beschreibung der Druck- und Luftmassenstromverteilung in natuerlich und maschinell gelueftetten Gebaeuden"
Fortschritts-Bericht der VDI-Zeitschriften, Reihe 6, Nr. 151, VDI-Verlags GmbH, Duesseldorf, (1984).

[4] Aynsley, R.M.; Melbourne, W. and B.J. Vickery:
Architectural Aerodynamics
Applied Science Publisher LTD, Barking, England, (1977).

[5] Davenport, A.G.:
"A Rationale for the Determination of Basic Design Wind Velocities"
ASCE *Proceedings* 86 (1960), pp. 36-68.

[6] Zuranzki, J.:
"Windbelastung von Bauwerken und Konstruktionen"
Verlagsgesellschaft Rudolf Mueller, Koeln-Braunsfels, (1969).

[7] Tamura, G.T. and Wilson, A.G.:
"Pressure Difference Caused by Chimney Effect in Three High-Rise Buildings"
ASHRAE Transactions, 73 (1967), Part II, pp. II.1.1-II.1.10.

[8] Tamura, G.T. and Wilson, A.G.:
"Building Pressures Caused by Chimney Action and Mechanical Ventilation"
ASHRAE Transactions, 73 (1967), Part II, pp. II.2.1.-II.2.12.

[9] Esdorn, H.:
"Luftdurchlaessigkeit der Fenster und Druckverteilung im Gebaeude"
In: Das Hochhaus der BASF "Planung, Ausfuehrung, Erfahrungen",
J. Hoffmann, Stuttgart, (1958).

[10] Brinkmann, W.:
"Zur Bestimmung des Lueftungswaermebedarfs hoher Gebaeude"

Doctoral Dissertation, Technische Universitaet Berlin, (1980).

[11] Kronvall, J.:
"Air Flow in Building Components"
Doctoral Dissertation, Lund Institute of Technology, (1980).

[12] McGrath, P.T.:
"The Prediction of Infiltration through Building Components; The Assembly of a Device to Measure Air Infiltration through Components with Suggested Method of Producing Data Which Could Be Used to Form the Basis of a Prediction Model"
Dissertation, University of Manchester, (1982).

[13] ASTM Standard E 779 - 81
"Measuring Air Leakage by the Fan Pressurization Method"
ASTM Committee E-6 on Performance of Building Construction, Philadelphia, (1981).

[14] Grimsrud, D.T., Sherman, M.H. and Sonderegger, R.C.:
"Air Leakage in a Building at Low Pressures Using an Alternating Pressure Source"
Kongressbericht XXI. Intern. Kongress fuer Technische Gebaeude-ausruestung, Teil 1, (1980), p. 124-127.

[15] Sherman, M.H.; Wilson, D.J. and Kiel, D.E.:
"Variability in Residential Air Leakage"
Proceedings, Symposium on Measured Air Leakage Performance of Buildings, ASTM, Philadelphia, (1984).

[16] Raisch, E.:
"Die Waerme- und Luftdurchlaessigkeit von Fenstern verschiedener Konstruktion"
GI Gesundheitsingenieur 45 (1922), p. 99-105.

[17] Reiher, H.; Fraass, K. and Settele, E.:
"Ueber die Frage der Luft- und Waermedurchlaessigkeit von Fenstern"
1. Teilbericht, Waermewirtschaftliche Nachrichten 6 (1932/33), pp. 42-59.

[18] Krischer, O. and Beck, H.:
"Die Durchlueftung von Raeumen durch Windangriff und der Waermebedarf fuer die Lueftung"
VDI-Berichte, Vol. 18, 1957, 29-59.

[19] Deutsches Institut fuer Normung. DIN 4701:
"Regeln fuer die Berechnung des Waermebedarfs von Gebaeuden"
Beuth Vertrieb Berlin, (1983).

[20] Feustel, H.E. and Lenz, Th.P.:
Patterns of Infiltration in Multifamily Buildings
Lawrence Berkeley Laboratory, Report No. LBL 17584, (1984).

[21] Feustel, H.E.:
"Multizone Infiltration Studies at Lawrence Berkeley Laboratory"
Proceedings, CLIMA 2000, Volume 6, Building Envelope Improvement, (1985).

[22] Feustel, H.E.;
Development of a Simplified Multizone Infiltration Model.
Lawrence Berkeley Laboratory, Report No. LBL 19095, (1985).

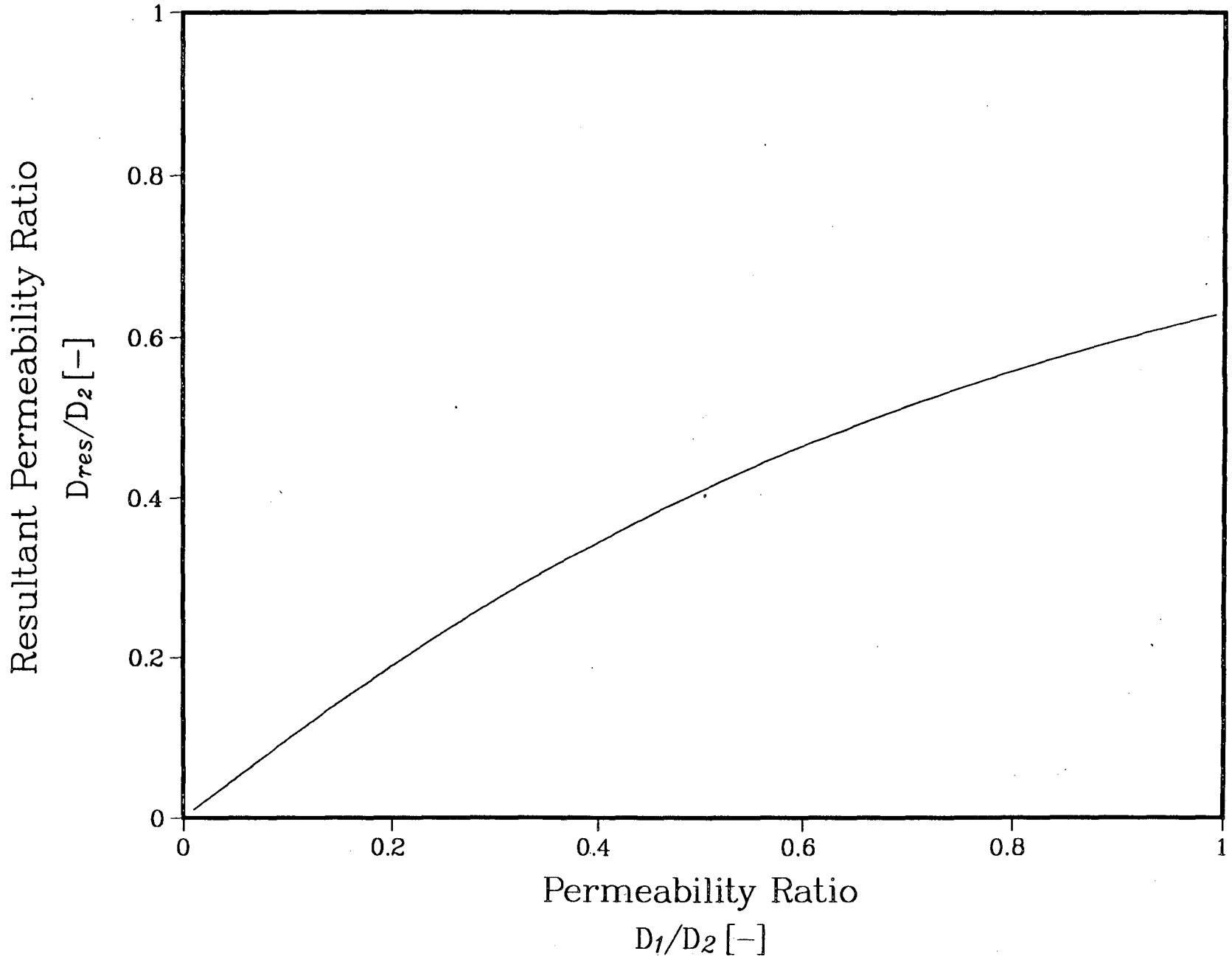

Fig. 1: Resultant Permeability Ratio vs. Permeability Ratio

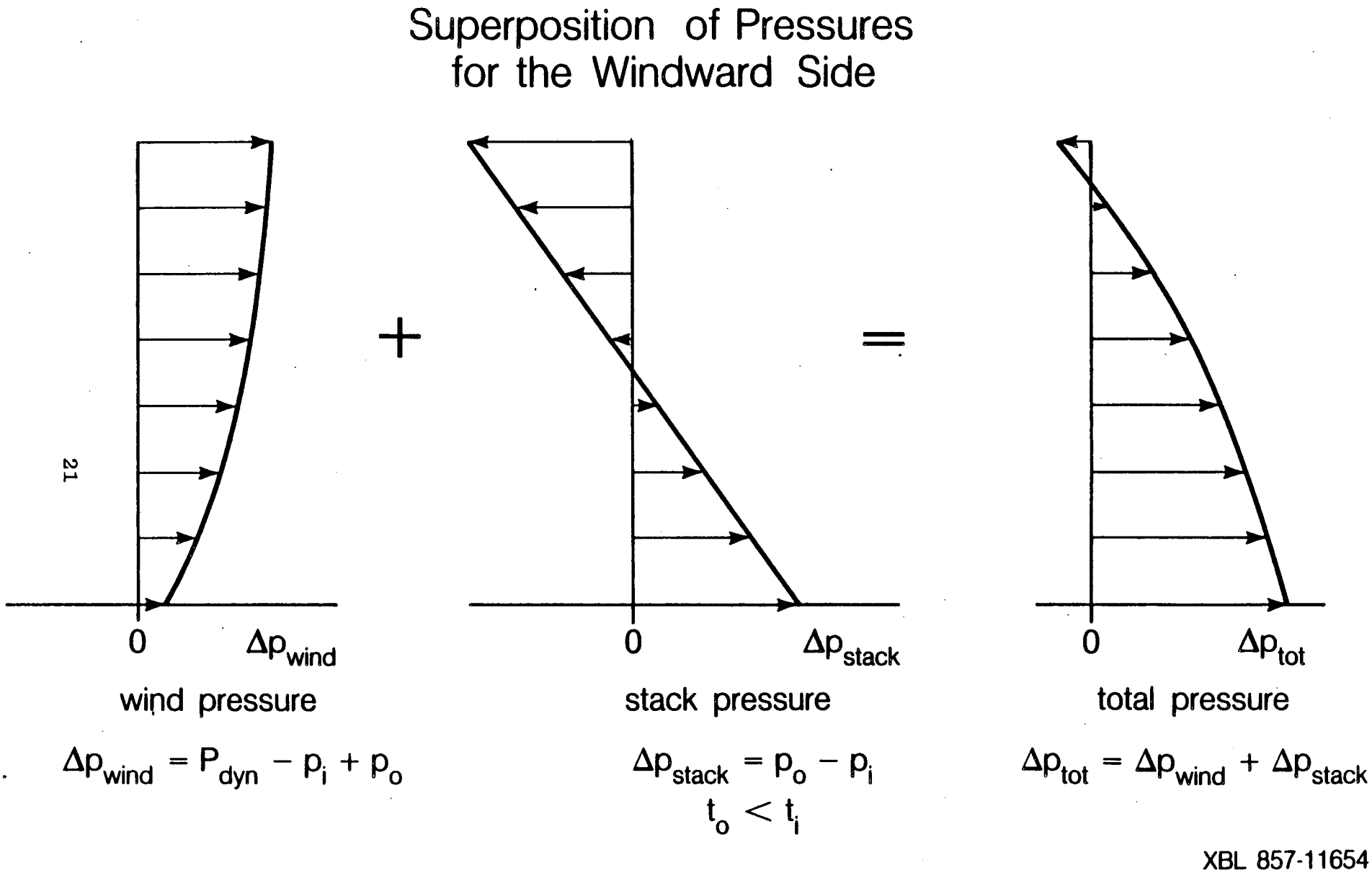

Fig 2: Superposition of Pressures for the Windward Side

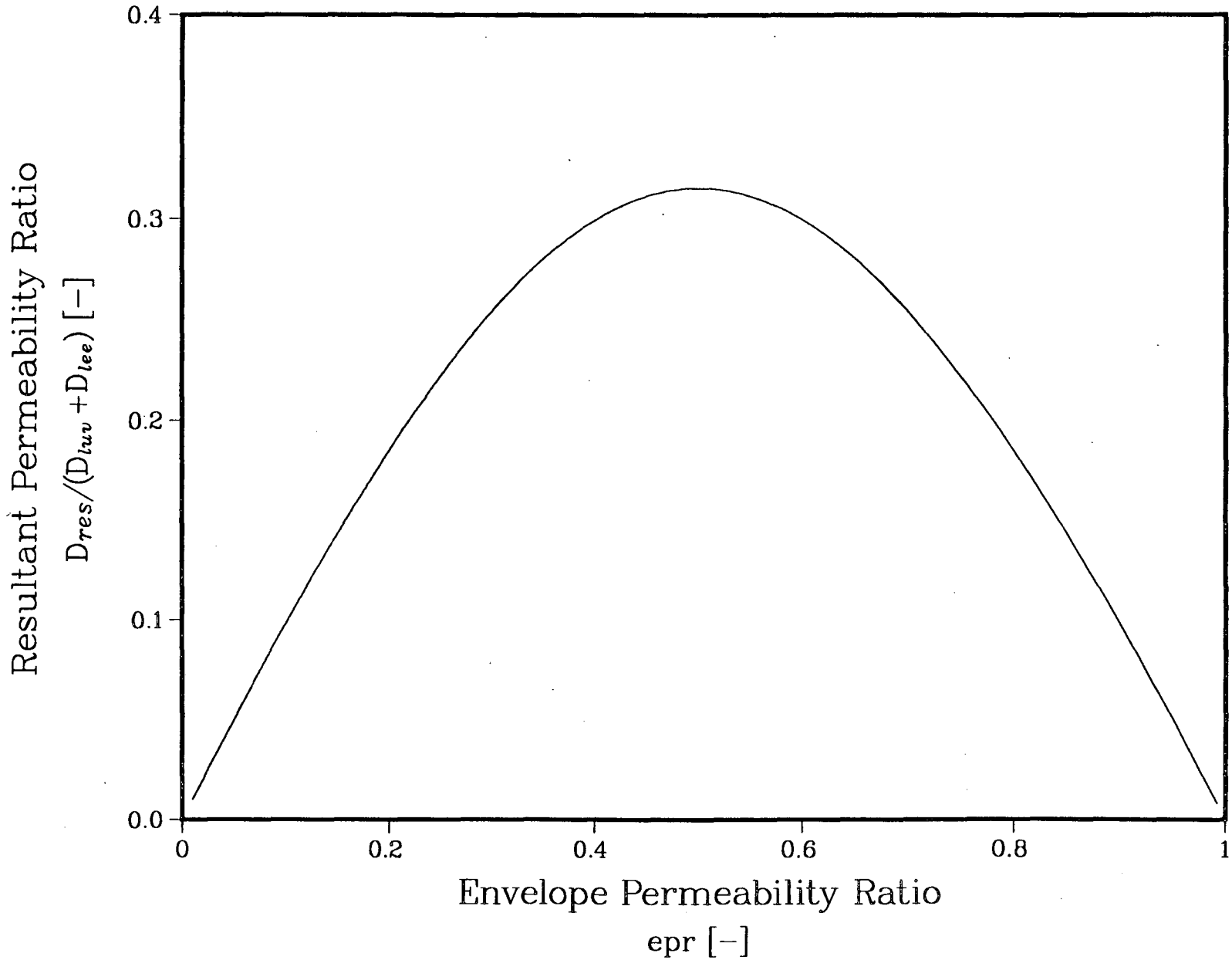

Fig. 3: Resultant Permeability Ratio vs. Envelope Permeability Ratio

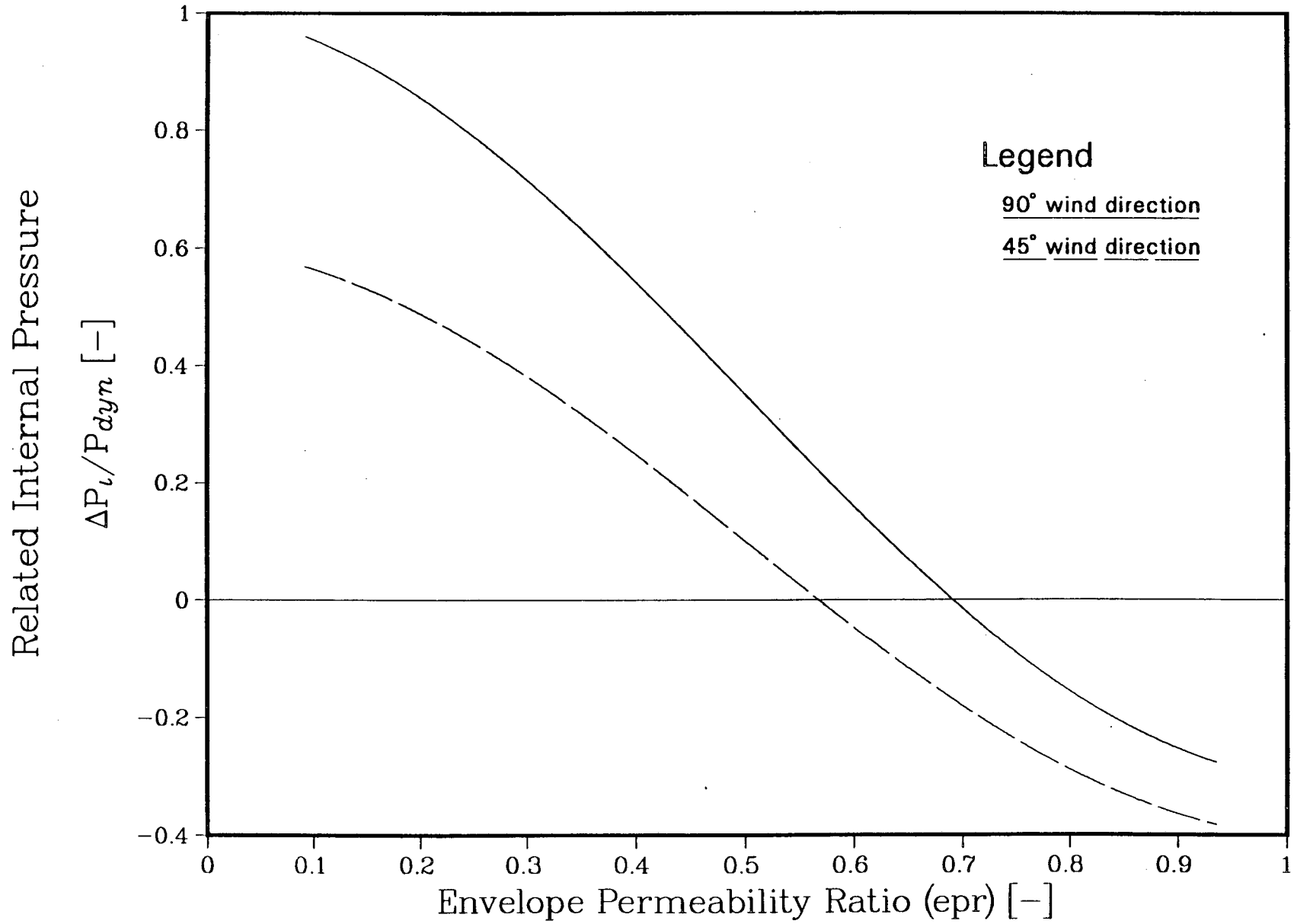

Fig. 4: Related Internal Pressure vs. Envelope Permeability Ratio

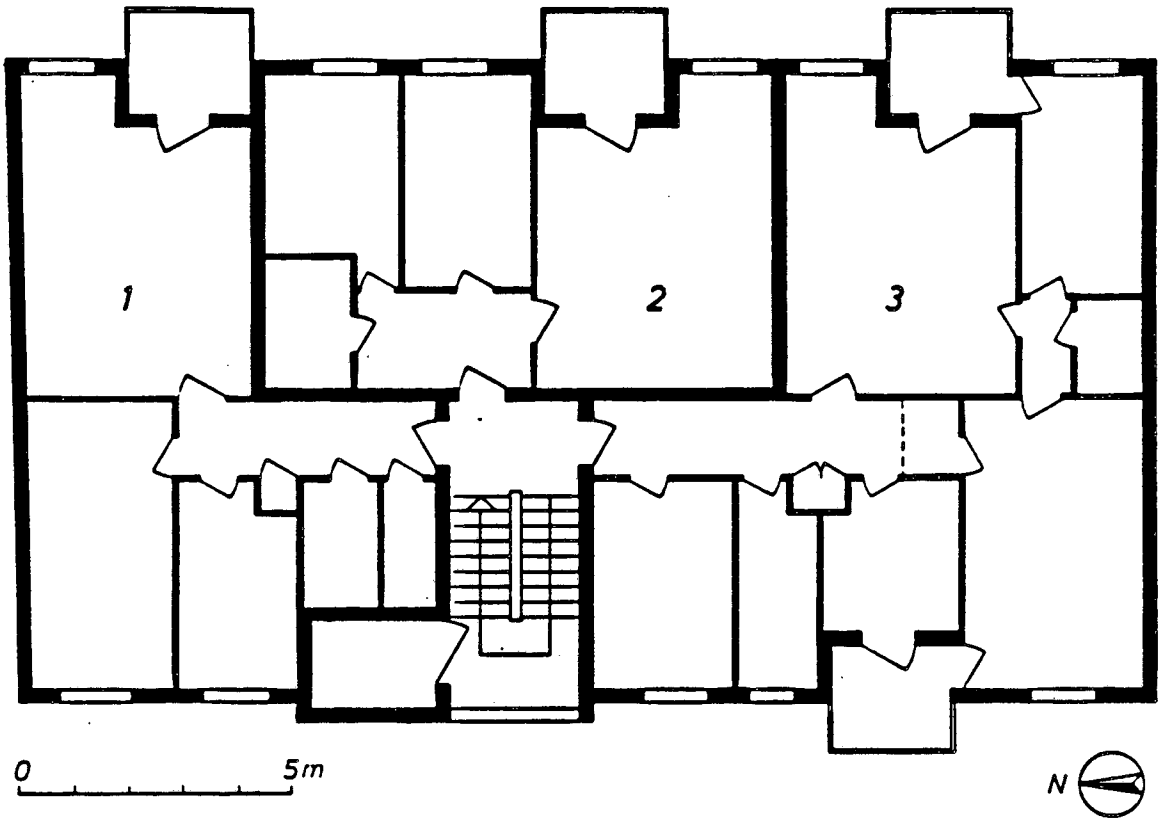

floor plan Brunsbuettler Damm 37

Fig. 5: Floor Plan "Brunsbuettler Damm 37"

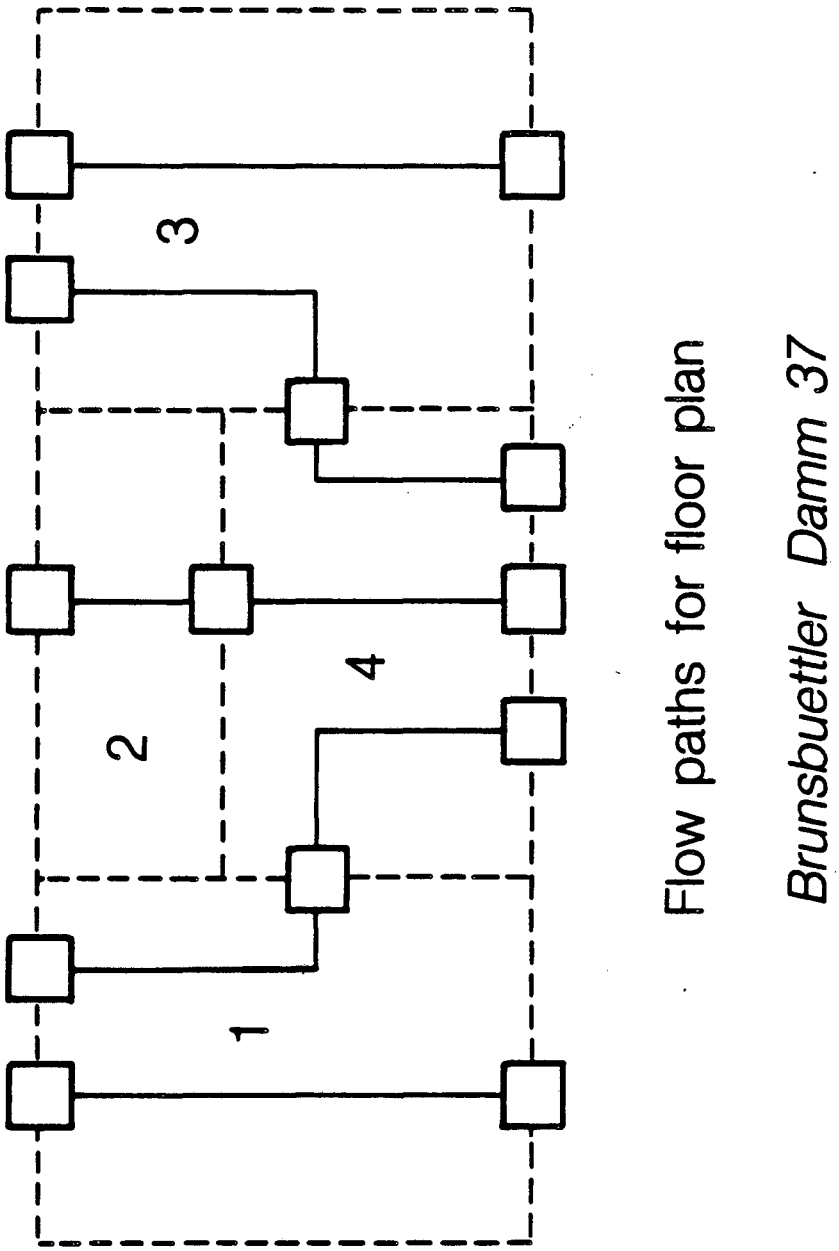

Fig. 6: Horizontal Air Flow Path for Floor Plan "Brunsbuettler Damm 37"

This report was done with support from the Department of Energy. Any conclusions or opinions expressed in this report represent solely those of the author(s) and not necessarily those of The Regents of the University of California, the Lawrence Berkeley Laboratory or the Department of Energy.

Reference to a company or product name does not imply approval or recommendation of the product by the University of California or the U.S. Department of Energy to the exclusion of others that may be suitable.

LAWRENCE BERKELEY LABORATORY
TECHNICAL INFORMATION DEPARTMENT
UNIVERSITY OF CALIFORNIA
BERKELEY, CALIFORNIA 94720